Melt Polycondensation of Poly(ethylene terephthalate) in a Rotating Disk Reactor

SEONG ILL CHEONG and KYU YONG CHOI*

Department of Chemical Engineering, University of Maryland, College Park, Maryland 20742

SYNOPSIS

A multicompartment model is proposed for a semibatch melt polycondensation of poly(ethylene terephthalate) in a rotating disk polymerization reactor and compared with laboratory experimental data. The reactor is a horizontal cylindrical vessel with a horizontal shaft on which multiple disks are mounted. The reactor is assumed to comprise N equal sized compartments and each compartment consists of a film phase on the rotating disk and a bulk phase in which disks are partially immersed. The effects of disk rotating speed, number of disks, reaction temperature, and pressure were investigated. It was observed that ethylene glycol is predominantly removed from thin polymer layers on the rotating disks and the enhanced interfacial area exerted by ethylene glycol bubbles accounts for about 30–50% of the total available interfacial mass transfer area. Although the rate of polymerization increases as more disks are used, the maximum number of disks in a reactor must be determined properly in order to prevent the formation of thick polymer films that result in a reduced specific interfacial area and reduced polymerization efficiency. At a fixed reaction pressure, the equilibrium conversion is reached but the rate of reaction can be further increased by increasing the reaction temperature. The results of the proposed multicompartment model are also compared with those predicted by a simple one-parameter model. © 1995 John Wiley & Sons, Inc.

INTRODUCTION

Many industrially important engineering thermoplastics such as poly(ethylene terephthalate) (PET) are manufactured by multistage semibatch or continuous flow polymerization processes. In the first stage of PET synthesis, bis(hydroxy ethyl) terephthalate (BHET) monomer is prepared with either dimethyl terephthalate (DMT) or terephthalic acid (TPA) as a starting material. BHET and low molecular weight oligomers are then polymerized in the second stage to a relatively low molecular weight at about 260–280°C and 10–30 mmHg in the presence of a catalyst such as Sb_2O_3. During the polycondensation, reaction by-product (ethylene glycol, EG) is removed to promote chain growth reactions. High molecular weight polymer (X_n = 80–100) is then produced in the third stage by applying a higher vacuum.

To obtain high molecular weight polymers in the third stage or finishing stage, it is important to remove EG effectively from the highly viscous polymer melt. Therefore, the design of a finishing polycondensation reactor is focused on increasing interfacial mass transfer area for the removal of volatile reaction by-products. A finishing polycondensation reactor usually consists of a high vacuum horizontal cylindrical vessel with a horizontal rotating shaft on which disks, cages, or shallow flight screws are mounted. Wiped film reactors are also used industrially. A variety of agitator and reactor configurations for the finishing melt polycondensation can be found in the patent literature.[1-4]

In a continuous finishing reactor, low molecular weight prepolymers are supplied to the reactor and as the polymer melt travels along the reactor, those attached to the rotating shaft provide a large interfacial area for the removal of EG. In a rotating disk reactor system that is considered in this work, a fraction of polymer melt in the bulk phase is dragged upward as the shaft rotates, forming a thin polymer layer or film on the disk surface. The polymer layer, after being exposed to a vapor phase for a short pe-

* To whom correspondence should be addressed.

Journal of Applied Polymer Science, Vol. 58, 1473–1483 (1995)
 CCC 0021-8995/95/091473-11

riod of time, is mixed again with the bulk polymer melt. Quite obviously, it will be important to understand the polymer layer formation and mixing and reaction phenomena as well as the effects of reactor design and operation parameters in such a reactor for optimal operation of the reactor.

In recent years, a large number of modeling works on the finishing stage of PET polymerization have been published in the literature.[5-12] However, little experimental studies have been reported. In our earlier work,[9,10] a two phase model was proposed for the finishing stage melt polycondensation. In the two phase model, it is proposed that the flow pattern of the melt phase in a continuous reactor is of the plug flow and that the vapor phase is well mixed. No distinction between the film phase and the bulk phase is made. Therefore, the polymer phase in the reactor is viewed simply as a mixture of both the film and bulk phases. The rate of mass transfer of the condensation by-products from the melt phase to the vapor phase is described through a single mass transfer parameter (k_La), where a is the specific interfacial area. For a given reactor configuration, the mass transfer parameter is determined by fitting the model simulation results with actual reaction data. Because the two phase model contains only one adjustable parameter, it is easy to use and the model itself is independent of the type of reactor being used. However, a major drawback of the two phase model is that the effects of actual reactor design and operating parameters such as agitator dimension and shaft rotating speed cannot be directly investigated. This is because these design and operational factors are lumped into a parameter, a, the specific interfacial mass transfer area that must be estimated from the experimental data.

In this article we propose a multicompartment model for a rotating disk semibatch polycondensation reactor to overcome the limitation of the two phase model (or single parameter model). The proposed model consists of a bulk phase and a film phase on the rotating disk surfaces. Unlike the two phase model described in the above, we can directly analyze the effects of disk rotating speed and the number of disks on the progress of the reaction and polymer molecular weight. The results of model simulations are compared with laboratory experimental polymerization data.

REACTION MODEL

In the synthesis of PET several functional end groups are present. They are the hydroxyethyl group, methyl ester group, carboxyl acid group, and diethylene glycol group. Because the polymerization is carried out at high temperature, these functional end groups react with each other and the reaction kinetics become quite complicated.[13-15] Some side products such as diethylene glycol, even in small quantity, can affect the quality of the final polymer product. However, in our reactor model, we shall consider the main polycondensation reaction only and the focus will be given only on how the polymer molecular weight development is affected by the reactor design and operating conditions. The polycondensation reaction is expressed by

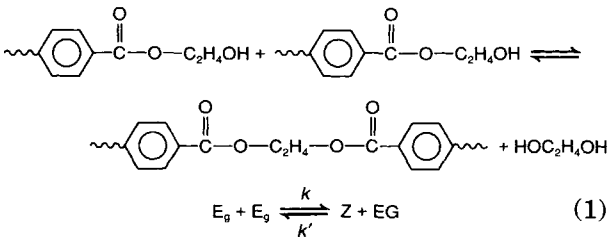

(1)

where E_g is the hydroxy ethyl group and Z the diester group. For the above reaction, the rate expression is given by

$$R_p = k[E_g]^2 - 4k'[Z][\mathrm{EG}]. \qquad (2)$$

Now, let us consider a horizontal cylindrical reactor vessel equipped with a horizontal shaft on which disks are mounted as depicted schematically in Figure 1(a). As the shaft rotates, a small amount of polymer melt is dragged upward from the lower bulk phase, forming a thin polymer layer on the surface of each disk and mixed again with the bulk polymer melt in the trough. Volatiles such as EG are removed from the polymer layer as it is exposed to the vapor phase. In a continuous rotating disk reactor, the bulk polymer melt flows in a transversal direction. In the semibatch reactor system considered in this study, there is no transversal flow. As vacuum is applied, condensation by-product (EG) diffuses from the polymer layer to the vapor phase. In modeling the reactor, it is thus necessary to consider both reaction and mass transfer from bulk and film phases.

For a semibatch polycondensation, this reactor system is modeled as shown in Figure 1(b). Here, the reactor is equipped with N equal sized disks that divide the whole reactor into N compartments. Each compartment consists of a vapor phase, a film phase on the disk, and a bulk phase in which a disk is partially immersed. In the absence of transversal flow, the rotation of plain circular disks may not

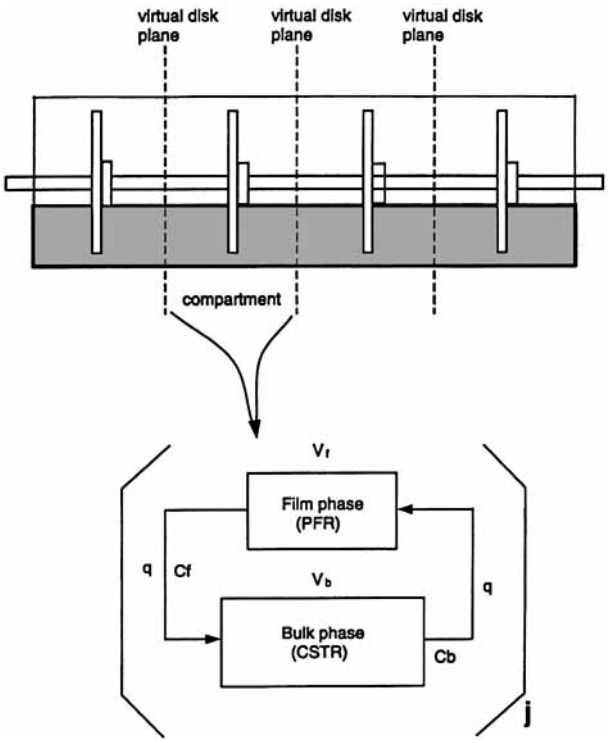

Figure 1 A schematic diagram of the multicompartment model.

provide a complete backmixing of polymer melt in the bulk phase. There is even a possibility that the polymer layers on the disks may not be mixed with the bulk phase and renewed completely. In our modeling, however, we assume that the bulk phase is well mixed with a continuous flow of polymer melt from and into the film phase on the rotating disk. It should be noted that this simplifying assumption may cause some discrepancies between the model and the data. The film phase on the disk, which is rotating at a constant speed, is assumed to be represented by a plug flow reactor model. It is further assumed that the mass transfer resistance at the phase boundary is present only in the polymer melt phase.

One of the key parameters in the proposed model is a specific interfacial area for mass transfer. As the polymerization takes place in both the bulk phase and the film phase, the total interfacial area must be known or estimated for the calculation of EG removal rate from the reactor. If a fraction of EG produced is present as small bubbles in the viscous melt phase, the total interfacial area for mass transfer will be much larger than that calculated from the geometry of the reactor and the disk.[12] However, it is practically very difficult to estimate how much bubbles are formed and what will be the interfacial area exerted by these bubbles. Thus, in our modeling, a combined value of mass transfer parameter $(k_La)_b$ is estimated for the bulk phase from experimental data. The mass transfer parameter for the film phase $(k_La)_f$ is estimated separately. In the mass transfer parameter expression, a is the specific interfacial area (cm^2/cm^3) that is dependent on the polymer holdup on the disk as well as the dimension of the disk or its wetted area. Thus, it is first necessary to know the polymer holdup on each disk for a given disk rotating speed and polymer molecular weight. To take the bubble formation effect, which is difficult to quantify through experimentation, into account, an empirical parameter f (mass transfer enhancement factor) is introduced. Here, f is defined as the ratio of the mass transfer parameter due to bubble formation to that without bubbles in the film phase. Thus, the overall mass transfer parameter in the film phase is given as $(1+f)(k_La)_f$. The parameter f can be calculated from the experimental data and one can quantify the effect of bubbles on the overall EG removal efficiency.

For the postulated reactor model shown in Figure 1, the dynamic reactor modeling equations take the following form.

Bulk phase:

$$\frac{d[E_g]_b}{dt} = -2r_b + \frac{V_f}{V_b t_r}([E_g]_f - [E_g]_b) \quad (3)$$

$$\frac{d[\mathrm{EG}]_b}{dt} = r_b - (k_La)_b([\mathrm{EG}]_b - [\mathrm{EG}^*]_b) + \frac{V_f}{V_b t_r}([\mathrm{EG}]_f - [\mathrm{EG}]_b) \quad (4)$$

$$\frac{d[Z]_b}{dt} = r_b + \frac{V_f}{V_b t_r}([Z]_f - [Z]_b). \quad (5)$$

Film phase:

$$\frac{d[E_g]_f}{d\tau} = -2t_r r_f \quad (6)$$

$$\frac{d[\mathrm{EG}]_f}{d\tau} = t_r\{r_f - (k_La)_f(1+f) \times ([\mathrm{EG}]_f - [\mathrm{EG}^*]_f)\} \quad (7)$$

$$\frac{d[Z]_f}{d\tau} = t_r r_f \quad (8)$$

where t_r is the surface renewal time determined by the disk rotating speed and $\tau (0 \le \tau \le t_r)$ the exposure time for the polymer film on a rotating disk to the

vapor phase. $\tau = 0$ is the time the disk departs the bulk melt phase. r_b and r_f represent the reaction rates in bulk and film phases, respectively. The initial conditions for the prepolymers (at $t = 0$) used in our model simulations are: $[E_g] = 0.921$ mol/L, $[Z] = 5.528$ mol/L, [EG] = 0 mol/L. For each reaction time interval (Δt), eqs. (3)–(5) are solved to calculate the bulk phase concentrations of functional end groups. Note that if the proposed model is applied to a continuous polycondensation reactor system, the feed concentration of EG is not zero. Because the volume of EG removed from the melt phase is very small in the finishing polymerization stage, we assume that the total volume of the polymer melt ($V_{\text{total}} = V_f + V_b$) is constant.

To calculate the specific interfacial area, the film thickness or polymer melt holdup on the disk must be known. In our previous experimental work[16] it was shown that the film thickness is not uniform in both radial and angular positions for low disk rotating speed. The film thickness depends upon the polymer molecular weight and the disk rotating speed. Figure 2 shows the film thickness profiles at various radial and angular positions for three PET samples of different molecular weight. At the shaft height (i.e., $\theta = 0°$), the film thickness increases in the radial direction. The polymer melt on the disk drains toward the center of the disk as it rotates due to gravity. In our model calculations, such film thickness nonuniformity is neglected and we assume that the film thickness is uniform. Then, the polymer layer thickness (h) on each disk is calculated by using the following correlation[16]:

$$T = 2.4 \times 10^{-5}\text{Ca}^{1.267}\text{Re}^{-1.362}\text{Fr}^{1.554}\Psi^{-2.839} \quad (9)$$

where T is the dimensionless film thickness $[h(\rho g/\mu r\omega)^{0.5}]$, Ca the capillary number $[\mu r\omega/\sigma]$, Re the Reynolds number $[\rho r^2\omega/\mu]$, Fr the Froude number $[r\omega^2/g]$, and Ψ the dimensionless radius $[r/R]$. r is the radial position, ω the disk rotating speed, and R the disk radius. The polymer melt holdup on a disk is calculated by

$$V_f = \int_{r_i}^{r_0} r\omega h\left(1 - \frac{\rho g h^2}{3\mu r\omega}\right) dr \quad (10)$$

where r_i is the inner radius of the wetted area and r_0 is the outer radius of the wetted area.

The vapor pressure of EG is calculated using the following equation[9]:

$$\ln P^0_{\text{EG}} = 49.703 - 8{,}0576.7/T - 4.042 \ln T \quad (P^0_{\text{EG}} \text{ in mmHg}, T \text{ in K}). \quad (11)$$

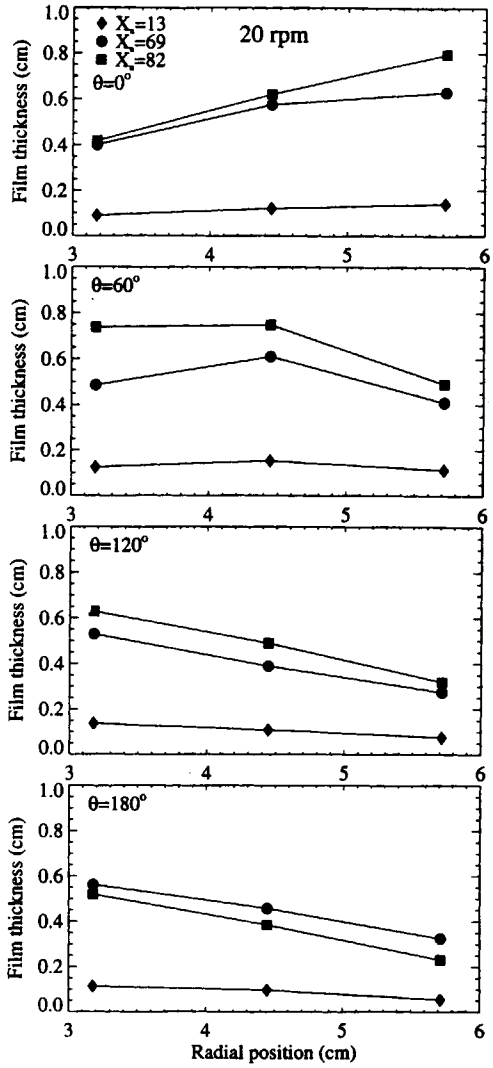

Figure 2 Polymer film thickness profiles on rotating disks.

The equilibrium mole fraction of EG at the interface is

$$X_{\text{EG}^*} = \frac{P}{\gamma_{\text{EG}} P^0_{\text{EG}}} \quad (12)$$

where P is the reactor pressure and γ_{EG} is the activity coefficient calculated using the Flory–Huggins model:

$$\ln \gamma_1 = \ln\left\{1 - \left(1 - \frac{1}{m}\right)\Phi_2\right\} + \left(1 - \frac{1}{m}\right)\Phi_2 + \chi\Phi \quad (13)$$

where subscripts 1 and 2 represent EG and polymer, respectively. Φ_2 is the volume fraction of polymer, χ the polymer–solvent interaction parameter ($\chi = 1.3$), and m the ratio of molar volumes of polymer to EG. Because the mole fraction of EG is very small, $\Phi_2 \approx 1$, and eq. (13) is reduced to

$$\gamma_{EG} = \frac{1}{m} \exp\left(1 - \frac{1}{m} + \chi\right). \quad (14)$$

Then, the interfacial concentration of EG is expressed as follows:

$$[EG^*] = \frac{C_{poly} X_{EG^*}}{1 - X_{EG^*}} = \frac{P[E_g]}{2(P^0_{EG}\gamma_{EG} - P)} \quad (15)$$

where $X_{EG^*} = P/P^0_{EG}\gamma_{EG}$. The degree of polymerization is given by

$$X_n = 1 + \frac{2[Z]}{[E_g]}. \quad (16)$$

The amount of EG removed from each compartment during the film exposure time t_r is given by

$$Q_{EG} = \int_0^{t_r} (k_L a)_f (1 + f)([EG]_f - [EG^*]_f) V_f + (k_L a)_b ([EG]_b - [EG^*]_b) V_b \, dt. \quad (17)$$

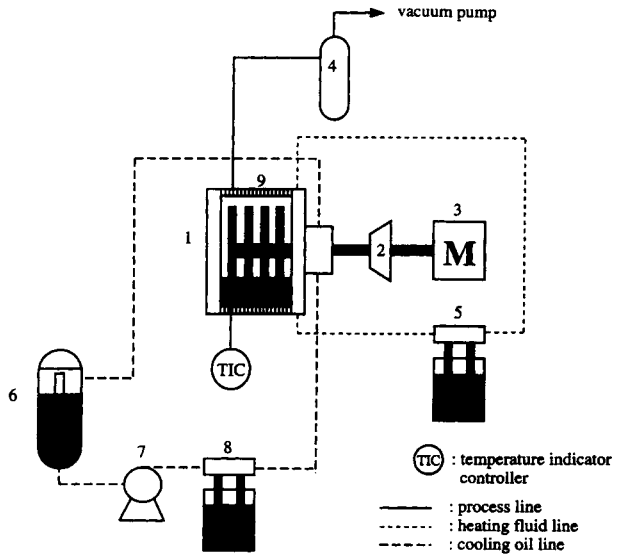

Figure 3 Experimental system for semibatch rotating disk melt polycondensation: 1, polymerization reactor; 2, motor speed reducer; 3, variable speed motor; 4, condensor; 5, circulating heating bath; 6, cooling oil reservoir; 7, cooling oil circulation pump; 8, refrigeration bath; 9, heating band.

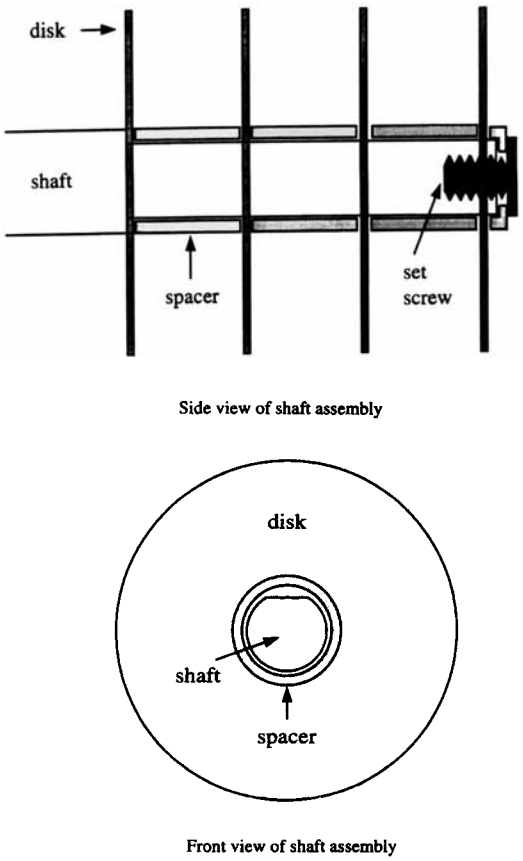

Figure 4 Layout of a rotating disk shaft assembly.

The mass transfer coefficient is given by $k_L = 2\sqrt{D/\pi t_r}$ where D is the diffusivity of EG in the polymer melt ($D = 1.6 \times 10^{-4}$ cm^2/s)[17] and the exposure time is calculated from the disk rotating speed.

EXPERIMENTAL

For semibatch polycondensation experiments, a bench scale rotating disk reactor device was built as shown schematically in Figure 3. This reactor was also used to measure the thickness of the film on a rotating disk.[16] The reactor ($D = 14.0$ cm) is made of stainless steel and disks ($D = 12.7$ cm) are mounted on a central shaft. The distance between the two neighboring disks can be adjusted by using a spacer. Depending on the length of the spacer, we can change the distance between the adjacent disks. In our reactor, up to 12 disks can be mounted on the shaft. Figure 4 shows the detailed layout of the shaft assembly.

The reactor is first charged with dried prepolymer pellets of known molecular weight (X_n = 13) and heated to a desired reaction temperature. No additional polycondensation catalyst is added. The polymer melt level is maintained 2 cm below the shaft height. When the desired temperature is attained, a shaft motor is started and the reactor pressure is gradually reduced to a desired pressure level. At every sampling time, a small amount of polymer is taken from the reactor for molecular weight analysis. EG removed from the reactor is condensed and its amount measured. The polymer molecular weight is measured by gel permeation chromatography (GPC) with a UV detector and chloroform containing 2 vol % hexafluoroisopropanol (HFIP) as a solvent. Four Ultrastyragel columns (Waters) were used. For GPC analysis, 5 mg of polymer sample was dissolved in 0.1 mL of pure HFIP. After complete dissolution, chloroform was added to 5 mL, and 5 μL of sample solution was filtered and injected into the column at 1 mL/min of solvent flow rate.

RESULTS AND DISCUSSION

In our experimental and modeling studies, we investigated the effects of disk rotating speed, number of disks, reaction temperature, and pressure on polymer molecular weight. Figure 5 shows the effect of disk rotating speed on the polymer molecular weight and the EG removal rate at 280°C and 0.5 mmHg with four disks in the reactor (or 0.26 disk/cm reactor). Here, the lines are model simulation results. The forward reaction rate constant used in the model calculations is $k = (9.77 \times 10^3 \pm 33)\exp[-(13.40 \times 10^3 \pm 3.785 \times 10^3)/T$(L/mol min)[18] and the equilibrium rate constant $K = 0.5$ is used.[5,8,9,19] The maximum disk rotating speed used in our experiments was 27 rpm. Figure 5 also shows the experimental results without disk rotation. The data obtained without disk rotation were used to estimate the bulk phase mass transfer parameter: at 0.5 mmHg, $(k_La)_b = 3.9 \times 10^{-3}$ (270°C), 4.2×10^{-3} (280°C), 5.3×10^{-3} (290°C); at 280°C, $(k_La)_b = 3.7 \times 10^{-3}$ (2.0 mmHg), 4.2×10^{-3} (0.5 mmHg), 4.6×10^{-3} (0.1 mmHg). Notice that without disk rotation, X_n increases from 13 to 24 in 2 h. As the disk rotates, the polymer molecular weight increases more rapidly. It is also seen that up to X_n = 50, the molecular weight increases almost linearly with reaction time. The bottom diagram in Figure 5 for the rotating disk cases indicates that the reaction has not reached its equilibrium after 2 h of reaction.

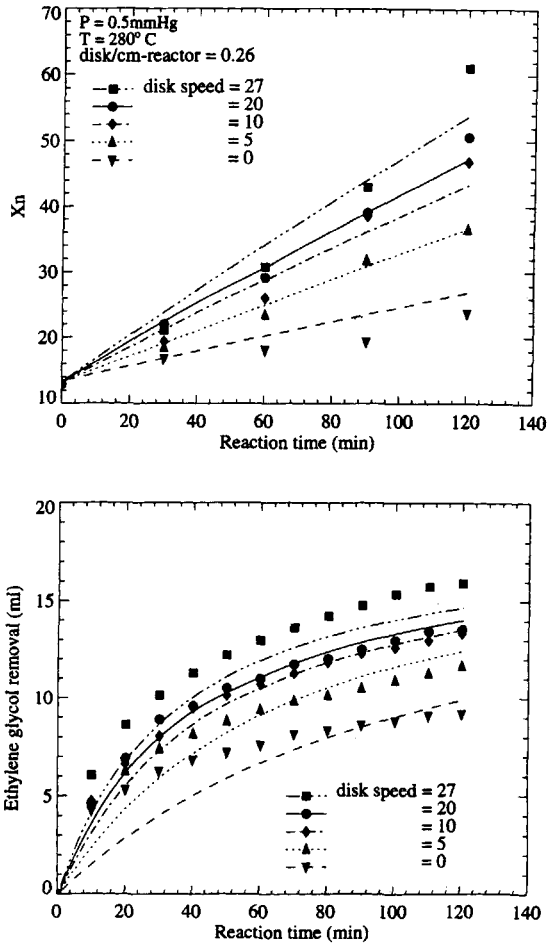

Figure 5 Effect of disk rotating speed on number average degree of polymerization (X_n) and ethylene glycol removal (symbols, data; lines, model calculations).

Figure 6 shows the variations in the overall film phase mass transfer parameter $[(1 + f)(k_La)_f]$, fractional melt holdup on the disks (V_f/V_{total}), melt viscosity, and f values for three different values of disk rotating speed during the reaction period (model calculations). As the reaction progresses, both melt viscosity and fractional melt holdup increase sharply. The mass transfer parameter in the film phase decreases with reaction because the specific interfacial specific area (a) for mass transfer decreases as the polymer melt holdup (or film thickness) on the disk surfaces increases (Figure 6(b)). For each experimental run, the mass transfer enhancement factor (f) due to EG bubbles was determined using the Rosenbrock's direct search optimal parameter estimation method to fit the experimental data of X_n (number average degree of polymerization) and EG removal rate. In our model

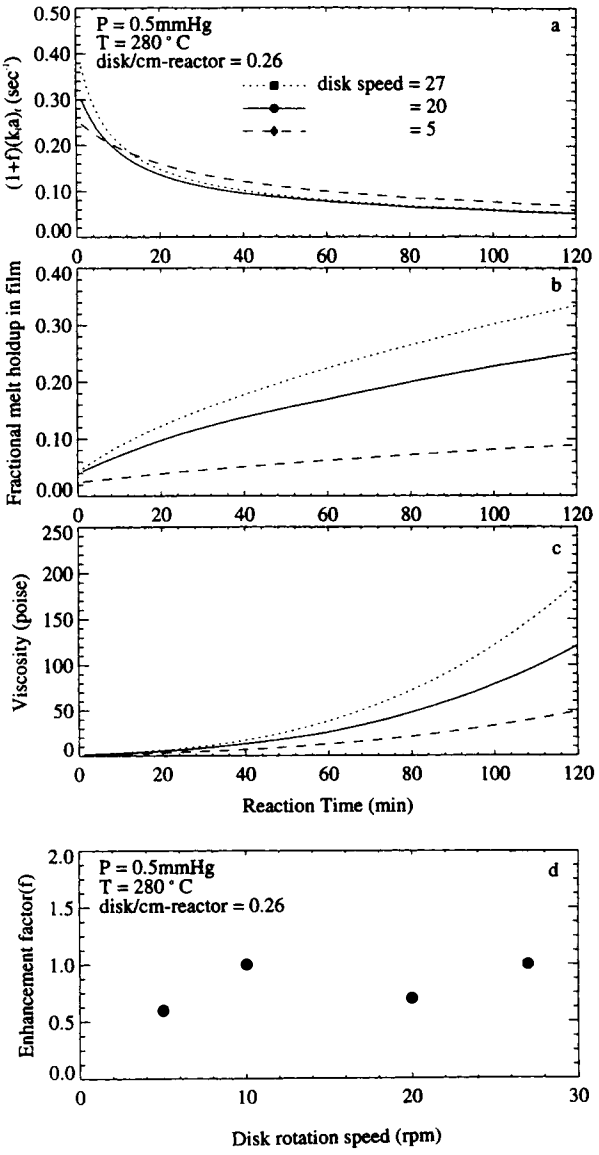

Figure 6 Profiles of overall film phase mass transfer parameter, fractional melt holdup in film phase, melt viscosity, and mass transfer enhancement factor (model calculations).

calculations, a constant value of f was used for the whole reaction period with fixed disk rotating speed, reaction temperature, and pressure. It is interesting to observe that the enhancement factor (f) is only slightly affected by the disk rotating speed and is in the range of 0.5–1.0 for the disk rotation speeds employed in our experimental work. This implies that the contribution of EG bubbles to the overall mass transfer from the polymer film phase is about 30–50%, which is quite significant. For a wiped film reactor system, Kumar et al.[8] report that a very high value of interfacial area must be used to obtain high molecular weight and that to accommodate such a large interfacial area, it is necessary for the film phase to have a large concentration of small bubbles of EG. Amon and Denson[11] calculated the interfacial area for a wiped film reactor by multiplying the actual geometric surface area by an arbitrary factor of 3 to account for the existence of small EG bubbles. It is also observed in Figure 6(a) that the mass transfer parameter values for the film phase are more than two orders of magnitude larger than that for the bulk melt phase.

Besides the mass transfer parameter (k_La), another factor that also affects the rate of removal of EG and polymer molecular weight is the interfacial concentration of EG. Figure 7 shows how the EG concentrations in the bulk phase and at the interface change with reaction at different disk rotating speed

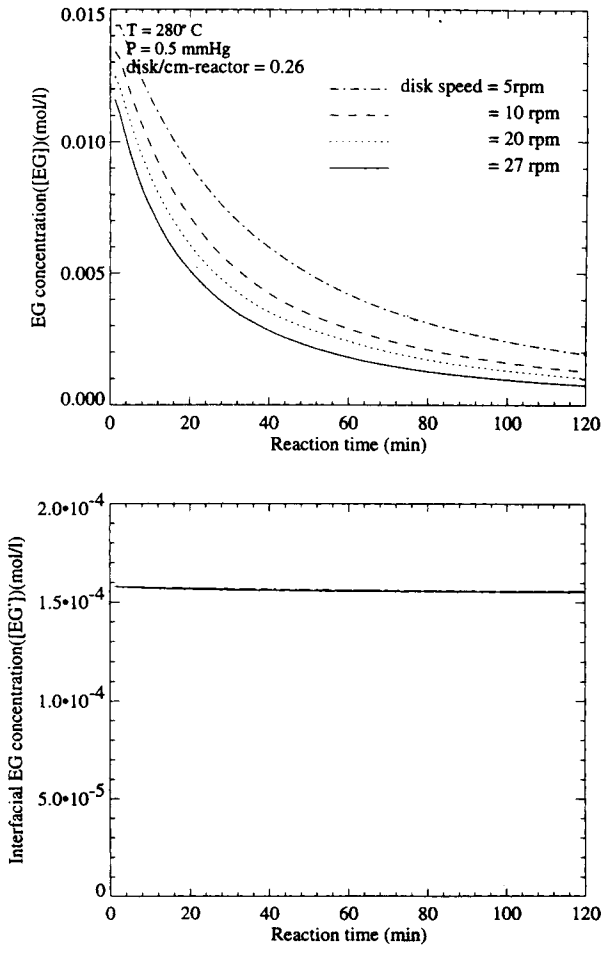

Figure 7 Ethylene glycol concentrations in bulk melt phase and at melt–vapor interface (model calculations).

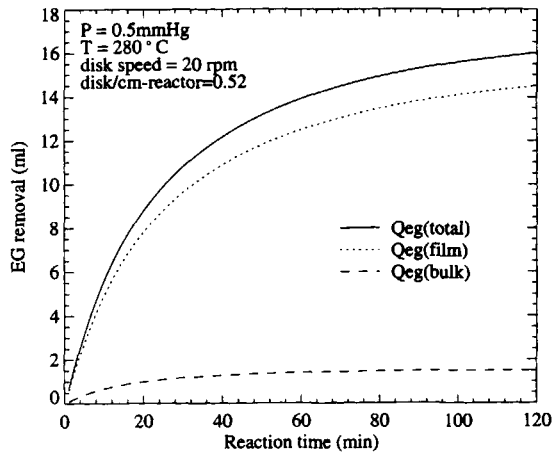

Figure 8 Ethylene glycol removed from film phase and bulk melt phase (model calculations).

(model calculations). For each case, the EG concentration in the bulk phase increases rapidly as the reaction starts (note: at $t = 0$, [EG] = 0) but decreases sharply during the initial reaction period and slowly approaches an asymptotic value. As expected, higher disk rotating speed or shorter exposure time (or more frequent surface renewal) results in a faster decrease in the bulk phase EG concentration. However, the EG concentration at the interface ([EG*]) is almost constant during the course of reaction as long as the reactor pressure is kept constant. Thus, the concentration driving force ([EG] − [EG*]) becomes smaller as the reaction continues.

The amounts of EG removed from the bulk phase and the film phase, respectively, are shown in Figure 8 for $N = 4$ where Q_{eg} is the amount of EG removed. Notice that the film phase mass transfer accounts for nearly 90% of the total EG removed from the reactor.

The number of disks is also an important reactor design and operating parameter. With more disks, the total mass transfer area increases for the removal of EG. However, there is a spatial limitation in the maximum number of disks a finite size reactor can accommodate. This is because as the polymer molecular weight increases, the thickness of a polymer layer increases; and if the distance between the adjacent disks is too small, these adjacent polymer layers stick together, reducing the effective interfacial area. Thus, the distance between adjacent disks must be determined properly and the maximum number of disks for a given reactor dimension must be chosen accordingly. Figure 9 illustrates the effect of disk numbers (or distance between the disks) on polymer molecular weight and EG removal rate at 20 rpm. Here, the lines represent the results of model calculations. The experiments were carried out with 4, 8, and 12 disks (or 0.26, 0.52, and 0.77 disks/cm reactor, respectively). It is seen that although the polymer molecular weight increases as more disks are used, polymer molecular weight does not necessarily increase in proportion to the number of disks being used. In Figure 10, the profiles of various parameters are illustrated. Notice that when $N = 12$ (0.77 disks/cm reactor), there is little bulk phase remaining after about 80 min of reaction, implying that the film thickness is very large. As a result, the specific interfacial area decreases and the efficiency of EG removal from the disk surfaces decreases dramatically. The calculated value of maximum film thickness after 100 min of reaction is 0.65 cm, indicating that the films on the two adjacent

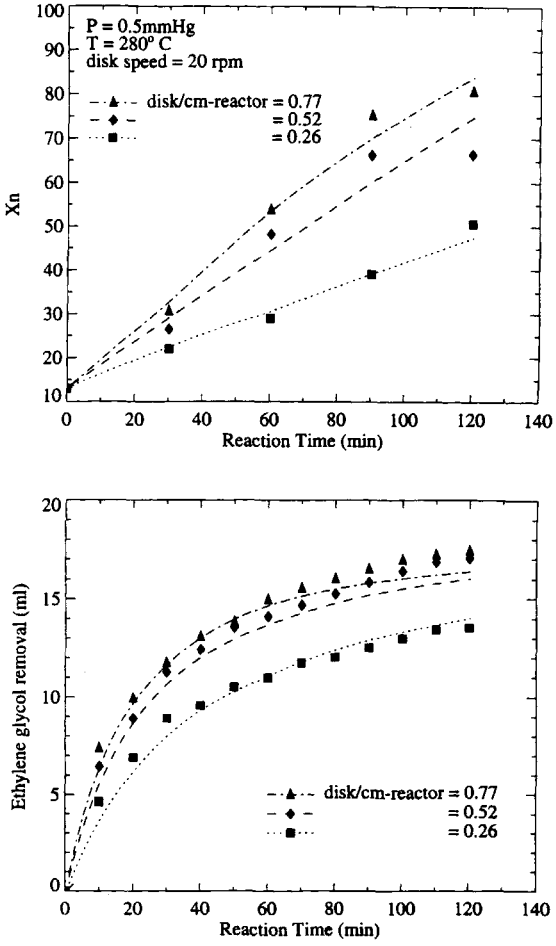

Figure 9 Effect of disk numbers: $N = 4$ (0.26 disk/cm reactor), 8 (0.52 disks/cm reactor), 12 (0.77 disks/cm reactor) (symbols, data; lines, model calculations).

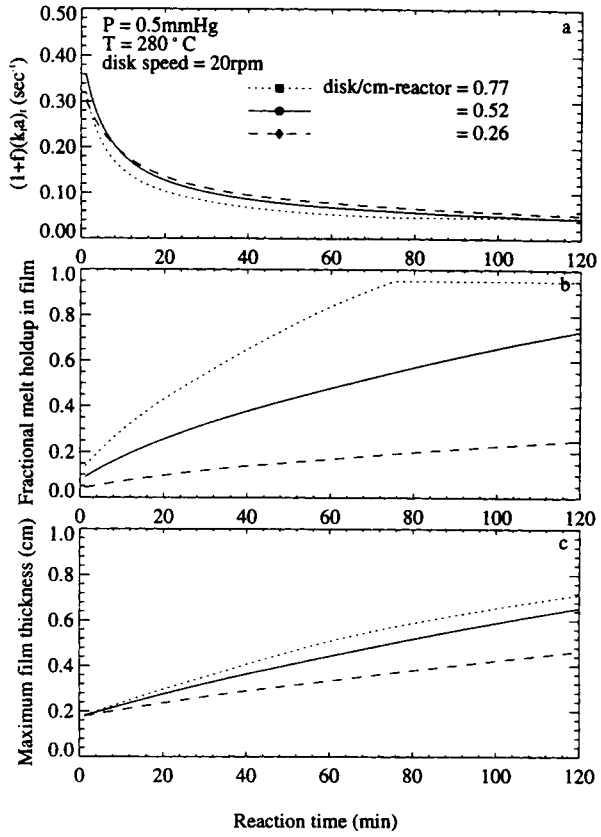

Figure 10 Profiles of overall film phase mass transfer parameter, fractional melt holdup in film phase, and maximum film thickness on a rotating disk (model calculations).

disks stick together, reducing the specific interfacial area significantly.

The effects of reaction temperature and pressure on X_n and EG removal rate are shown in Figures 11 and 12, respectively, for N = 4 and 20 rpm (lines − model calculations). Figure 11 indicates that raising the reaction temperature from 280 to 290°C has a strong affect in increasing the polymer molecular weight whereas reducing the pressure from 0.5 to 0.1 mmHg has only a marginal effect (Fig. 12). The interfacial EG concentration decreases from 6.3 × 10^{-4} mol/L at P = 2.0 mmHg to 0.37 × 10^{-4} mol/L at P = 0.1 mmHg; however, the contribution of the concentration driving force ([EG] − [EG*]) to the overall EG removal is far smaller than that of the overall mass transfer parameter. As a result, the most effective way to further increase the polymer molecular weight is to increase the reaction temperature instead of further reducing the reactor pressure. It should also be noted that higher reaction temperature may favor the formation of some side products.

Comparison with One Parameter Model

As mentioned earlier, the multicompartment model proposed in this study was developed to overcome the drawback of the one parameter model (or two phase model)[9,10] where a single mass transfer parameter is used to calculate the rate of EG removal. Recall that the geometric surface area and the interfacial area exerted by small EG bubbles are incorporated into a single parameter a (specific interfacial area) in the one parameter model. No distinction between the bulk phase and the film phase is made. We have applied the one parameter model to our experimental data and estimated the overall mass transfer parameter. Figure 13 shows the ex-

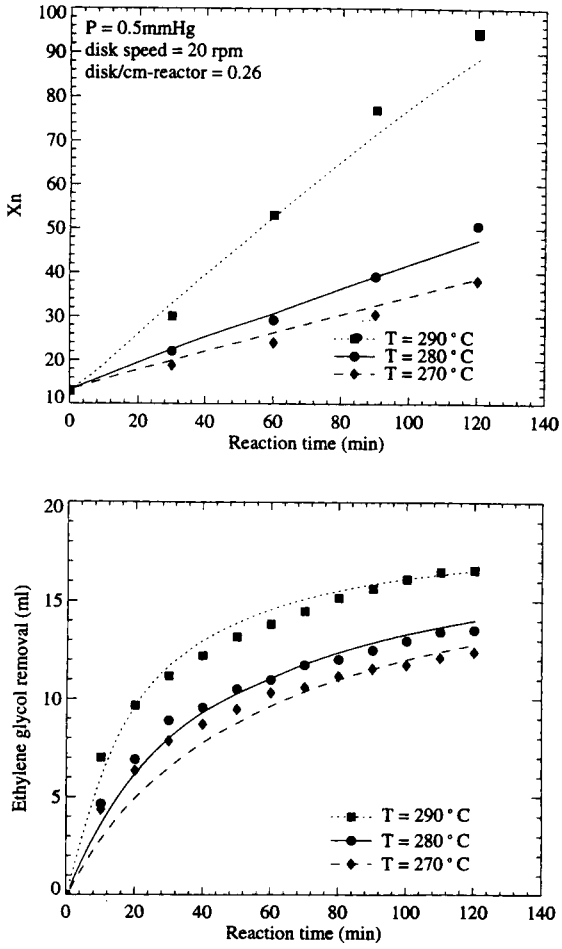

Figure 11 Effect of polymerization temperature (symbols, data; lines, model calculations).

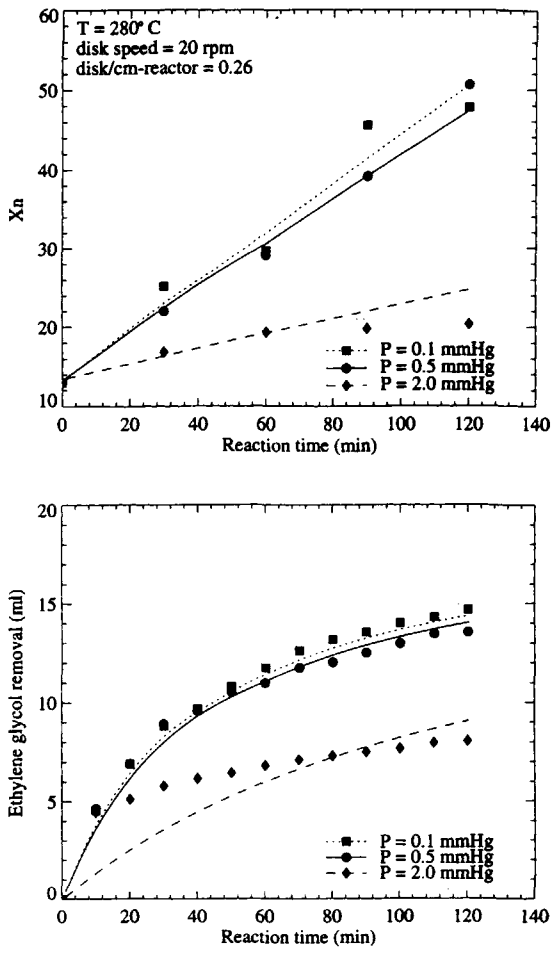

Figure 12 Effect of pressure (symbols, data; lines, model calculations).

perimentally observed X_n and the amount of EG removed as well as the predictions by the two models. It is seen that both models fit the experimental data reasonably well. Figure 14 shows the fractional melt holdup on the disks (calculated) and the mass transfer parameter values used in the two different models. Here, because the specific interfacial area changes during the course of reaction, average mass transfer parameter values are shown for the multicompartmental model. It is interesting to observe that the overall mass transfer parameter value for the one parameter model lies between the overall film phase mass transfer parameter and the bulk phase mass transfer parameter values. It must be reiterated that unlike the simple one parameter model, the effects of reactor design and operation parameters on the progress of polymerization can be directly examined by the proposed multicompartmental model.

CONCLUDING REMARKS

A multicompartmental model was proposed for semibatch melt polycondensation of poly(ethylene glycol) in a rotating disk reactor. The specific film phase interfacial area is calculated using an empirical correlation. The effects of disk rotating speed, number of disks in the reactor, reaction temperature, and pressure were investigated. It is shown that EG is mostly removed from thin polymer films on the rotating disks. The contribution of EG bubbles to the overall mass transfer efficiency is accounted for by introducing an empirical mass transfer enhancement factor f. The model calculations indicate that about 30–50% of EG removed from the film phase is due to the presence of EG bubbles. It has also been shown that the EG concentration gradient at the interface is not as important as the total inter-

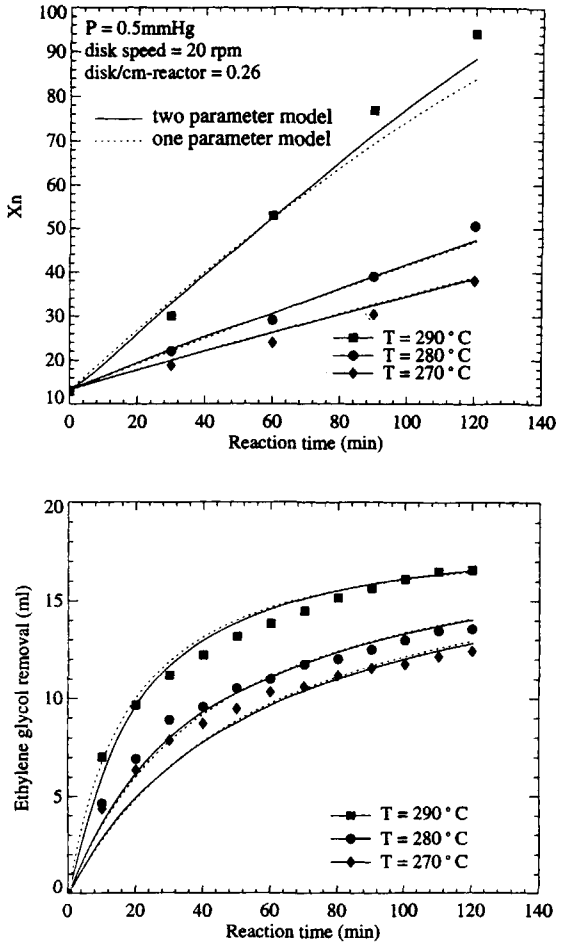

Figure 13 Comparison of one parameter model (two phase model) and two parameter model (multicompartment model) (symbols, data; lines, model calculations).

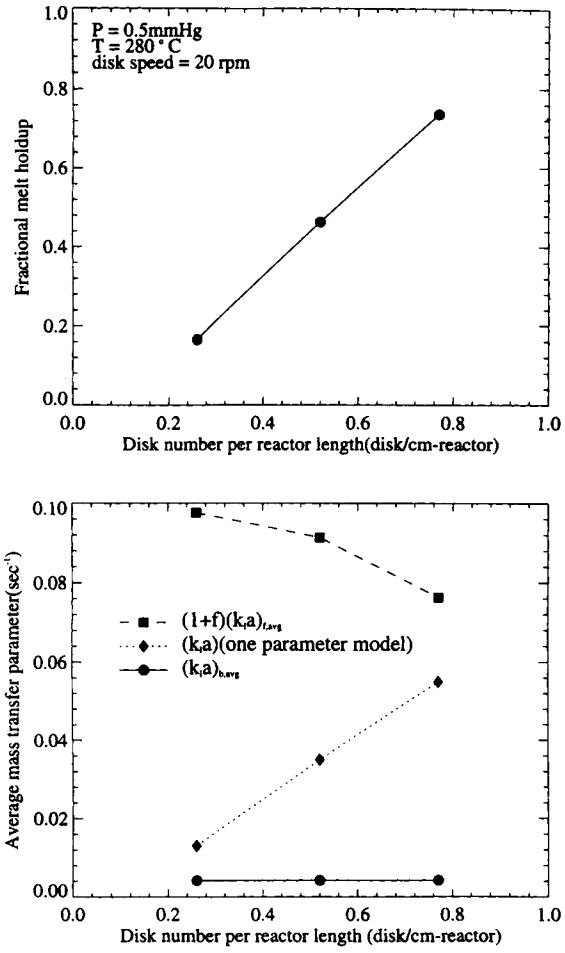

Figure 14 Fractional melt holdup and average mass transfer parameters used in one parameter model and two parameter model (multicompartment model) (model calculations).

facial area or mass transfer parameter value. In the pressure range studied (0.1–2.0 mmHg), increasing the reaction temperature is found to be more effective in increasing the polymer molecular weight than further decreasing the reactor pressure. For the experimental conditions employed in this work, the agreement between the model predictions and experimental data seems reasonable. Although it is not quite possible to identify the sources of model–data discrepancies at this point, it is believed that several assumptions made in our modeling might have caused them: for example, complete renewal of polymer layers on the disk when mixed with bulk polymer melt, uniform film thickness, constant value of mass transfer enhancement factor due to EG bubble formation, and perfectly mixed bulk phase where the only mechanism for mixing is the rotation of disks. More studies are desirable in the future to improve our understanding of these phenomena.

We are grateful for the financial support of the National Science Foundation (CTS 9209187) and the donation of prepolymer samples by Eastman Chemical Co. (Kingsport, TN).

REFERENCES

1. J. E. Crawford, R. W. Edwards, E. D. Hease, and W. C. L. Wu, U.S. Pat. 3,619,145 (1971).
2. M. Hachiya, K. Hiratsuka, and H. Fukumori, U.S. Pat. 3,532,151 (1970).
3. L. L. Kilpatrick, U.S. Pat. 3,248,180 (1966).
4. K. Ogata, K. Kazama, S. Suzuki, and Y. Morimatsu, U.S. Pat. 3,442,868 (1969).
5. K. Ravindranath and R. A. Mashelkar, *Polym. Eng. Sci.*, **22**, 628–636 (1982).
6. K. Ravindranath and R. A. Mashelkar, *AIChEJ.*, **30**, 415–422 (1984).
7. A. Kumar, S. K. Gupta, A. Ghosh, and S. K. Gupta, *J. Appl. Polym. Sci.*, **29**, 3217–3230 (1984).
8. A. Kumar, S. K. Gupta, S. Madan, N. G. Shah, and S. K. Gupta, *Polym. Eng. Sci.*, **24**, 194–204 (1984).
9. C. Laubriet, B. LeCorre, and K. Y. Choi, *Ind. Eng. Chem. Res.*, **30**, 2–12 (1991).
10. H. Castres Saint Martin and K. Y. Choi, *Ind. Eng. Chem. Res.*, **30**, 1712–1718 (1991).
11. M. Amon and C. D. Denson, *Ind. Eng. Chem. Fundam.*, **19**, 415–420 (1980).
12. G. Rafler, G. Reinisch, E. Bonatz, H. Versaumer, H. Gajewski, H. D. Sparing, K. Stein, and C. Muhlhaus, *J. Macromol. Sci.-Chem.*, **A22**, 1413–1427 (1985).
13. K. Ravindranath and R. A. Mashelkar, *Chem. Eng. Sci.*, **41**, 2197–2214 (1986).
14. K. Ravindranath and R. A. Mashelkar, *Chem. Eng. Sci.*, **41**, 2969–2987 (1986).
15. G. D. Lei and K. Y. Choi, *J. Appl. Polym. Sci.*, **41**, 2987–3024 (1990).
16. S. I. Cheong and K. Y. Choi, *J. Appl. Polym. Sci.*, **55**, 1819–1826 (1995).
17. T. M. Pell, Jr. and T. G. Davis, *J. Polym. Sci.: Polym. Phys.*, **11**, 1671–1682 (1973).
18. S. I. Cheong, Ph.D. Thesis, University of Maryland, 1994.
19. C. M. Fontana, *J. Polym. Sci., A-1*, **6**, 2343–2358 (1968).

Received January 23, 1995
Accepted May 28, 1995